ingegneria sismica
International Journal of Earthquake Engineering
Anno XLIII - Num. 2 - 2026

Graph Neural Network-Based Topology Modeling and Precise Fault Localization for Mobile Optical Cable Networks

Weishan Zhao[1], *Puyu Liu*[1,*], *Ming Li*[1], *Yong He*[1] *and Songjia Liu*[1]

[1] State Grid Zigong Electric Power Supply Company, State Grid Sichuan Electric Power Company, Zigong, Sichuan, China

SUMMARY: *This paper focuses on addressing mobile communication fault repair within an electric-power Communication network in State Grid Zigong; that is, a long-standing problem of delay in transferring faults due to the traditional paper-tickets system. A project-based repair system, which integrates topological Reasoning and online Workflow Control technologies to build a mobile application of the iStateGrid platform. A Mobile Optical Cable Graph Neural Network (MOC-GNN) was proposed to represent cable segments, optical Distribution frames, Devices, Service Paths, Repair Tickets, Roles, Telemetry windows as type Nodes, Model serviceTraversal, physical adjacency, Ticket Transfer, Authorisation, Alarm Propagation, Image Evidence, Historical Co-failure as typed Edges. Using a project-aligned digital-twin dataset with 18,240 fault events, 61,800 normal windows, 124 access rings, and 4,812 service paths, the model achieves 93.8% top-1 localization accuracy, 98.4% top-3 accuracy, 92.4% macro-F1, 78 m median error, and 226 m 95th-percentile error, outperforming rule-based, CNN, XGBoost, GAT, R-GCN, and HGT baselines. Approximately a 64% reduction in the average ticket-leave waiting time after adopting the new work-flow plan. The ablation results show that service-path relationships primarily impact the accuracy of localisation; The other features inRBAC, OCR, NLG, signatureandRedis-state contribute to improved compliance,ticket confirmation, report receipt and mobility-related aspects. The results support deployment of the micro-application as a topology-intelligent repair system rather than a simple electronic ticket tool.*

KEYWORDS: *Mobile repair Micro-Application, Optical Cable Communication Fault, Graph Neural Network, TMS2.0, Role-Based Access Control.*

1 Introduction

Electricity-poor Communication repairs need to be coordinated rapidly by on-call personnel, technicians, responsible persons, and site workers. In the paper-ticket procedure, fault evidence, approval, signatures, and restoration reports all require manual copy-paste operations, phone verification, and off-line transmission to extend handling time, reduce field accuracy, obscure the situation of repairs, etc. This research studies the mobile application of fault repair for the State Grid Zigong power supply company. Online fault transfer, on-site ticketing, the collection of signatures, structured record preservation, as well as subsequent statistical validation. It has a technical stack of workflow-engine control, RBAC (Access Control), dynamic authorization, OCR, NLG, TMS2.0 data re-use, Redis cache, mobile signature capture, etc. Therefore, the research subject is a problem of topology reasoning combined with repair-process control rather

*liupy151x@163.com
https://doi.org/10.65102/is2026778
Published: 30 April, 2026

than fault isolation.

There is a problem with alarm information, the location of repair work orders, workflow states, roles permissions, and field evidence all belonging to different types of repairs within one operation process. An alarm may appear at a device port, whereas repair is executed at a cable section, splice closure, ODF, or field cabinet. Ticket transfer is based on the authority, work process status, etc. Signature validity depends on signer identity, role, time, and ticket status. Based on the consistency of topological position, fault phenomena, corrections, and closure evidences during report generation. Previous research has enhanced detection capabilities, reasoning about causes of failures, soft-failure localization techniques, and topological-based prediction [1-12] but is still mainly focused at the network level. Approval Logic, Ticket Fields, Field Images, Signature Validity, Role-Constrained Actions are typically not located in a single Diagnostic Structure together. Mobile repair Systems generally digitise work process, but localisation is still carried out manually [13-20]. There is an actual gap between fault diagnosis and controlled repair operation implementation.

This paper tries to fill this gap by developing a graph-neural-network-based topology modelling and precise fault-location method for the mobile-optical fibre-repair micro-applications. A heterogeneous graph is generated based on the communication topology, TMS-2.0 resource records, repair tickets, field pictures, signatures, roles and telemetry windows. Based on the above design of relation-aware graphs for locating faulty cable segments and estimating their positions within these regions; Meanwhile, incorporating service traversal, ticket transfer and permission relationship data. The model is embedded directly in the mobile workflow to achieve dynamic authorisation, OCR-assisted field processing, NLG-generated reports and signature verification all work within this same graph topology. Evaluation focuses on the consequences of repairs rather than predictions solely; it includes candidate ranking, route-distance error, ticket-booking time, evidence completeness, authorization consistency, microservices latency, robustness, ablation test, and case-level traceability [21, 22].

The study is deliberately limited to the repair micro-application. To achieve that the user can see whether fault location, ticket status, evidence completeness, and authorisation information are available after each new valid operation. Avoiding the separation of algorithms and execution fields. A localisation result that fails to attach it to a ticket, route to the right person, or verify with mobile evidence is unsatisfactory for this project. A mobile form that lacks topology reasoning merely speed up circulation but cannot resolve the slowest diagnostic phase. Therefore, for similar reasons, alarms, work orders, images, signature information, topology objects, workflow states are regarded as related graph objects of a single repair process.

Another problem is that the field data are incomplete and asynchronous. Trace evidence can be later than the alarm; Images may come earlier than signs; TMS2. 0 records are later than temporary route adjustments; Redis status is earlier than stable work-order tables. Thus, the proposed graph adds evidence mask cells and workflow state nodes to ensure partial validity in generating ranked candidate sets and clearly marks absent fields. Lack of a differentiation between algorithmic confidence and process consistency. High-localization-confidence tests need to be quick; but the approvals and signatures are not abolished. Low confidence should not prohibit repair if the top three candidates still constitute an effective local inspection area. Then, evaluate the model in both scenarios of automatic-dispatch and assisted-diagnosis separately.

Thereafter, the content will remain similar to this. Methods Constructs the heterogenous repair graph and defines a relation-aware message-passing model along with the RBAC-constrained workflow-action head. Localisation accuracy; Repair time reduction; Robust to missing evidence; Module contribution analysis; Microservices scalability tests; Case-level traceability verification results. The Conclusion defines the Value and deployment range of

graph-based intelligent recognition in the mobile communication fault-finding microapplication.

2 Methods

2.1 Project-Oriented Data Organization and Heterogeneous Repair Graph Construction

Based on the project-based organisation of organisational data. The mobile repair micro-application must support online fault reporting, approval, field handling, signature, closure, and statistical analysis. Therefore, the data layer of alarm record storage is not sufficient. Five data sources are organised [23-25]. The first one is the TMS2.0 resource database that includes Communication Device Identifiers, Optical Cable Sections, Optical Distribution Frames, Ports, Service Paths, Topology Positions and Resource Ownership. The second one is the Work-Order Database, which contains details such as repair ticket's own condition (initiator, Reviewer), Approval Status, Historical Repair Time; Thirdly, there are mobile terminal records that include field images, OCR processing results, signatures with trajectory recognition, pressures-aware handwritten texts, and time-stamped operations. The fourth one is telemetry and alarm information, such as receive-optical-power detection; Bit-err rate drift test; Unavailable Seconds; Protection-switching times counted; Alarm Age;OTDR-like trace function. The fifth one is a micro-service Operation log, which includes APIs, message Pushs, Authorization decisions, Redis's hit rate and workflow Node transitions.

The repair object is organised as a heterogeneous graph rather than a table. The structure of a Table can accommodate tickets; however, it lacks information that one ticket is linked to a Service Path; the path passes through multiple Cable Sections, which are shared by those sections at an Optical Distribution Frame, and only the site-signer has authority in a certain Ticket Status. Contains physical plant nodes, communication service nodes, repair workflow nodes, role nodes and evidence nodes in the graph. Physical plant nodes refer to cable segments, optical Distribution Frames (OFFs), Field Cabinets, Ports, aggregation devices, and Base Station/terminal Communication Access Points. Service Nodes contain transport service paths and backup Paths. The workflow nodes are fault report, technical review, leader approval, repair ticket, field signature, restoration check-out, and ticket closure. Role nodes involve duty personnel, technical specialists, responsible leaders, repair teams, work Leaders and issuers. Evidence Nodes consist of alarm Windows, trace events, fault Images, OCR Fields, NLG Report Drafts, and Signature Samples.

A diagnosis-and-repair Window is given by way of a definition in this project.

$$G_\tau=(V,E,R,X_\tau,S_\tau),\quad E=\{(u,r,v)\square u,v\square V,\ r\square R\}. \tag{1}$$

Here, G_τ is the heterogeneous graph of window (τ); V is a node set; E is a typed edge set; R is a relation-type set; The feature matrix based on topological structure, telemetry, tickets, OCR and mobile operations data is X_τ. S_τ is a workflow-state vector. The relation set consists of physical adjacency, service traversal, alarm propagation, ticket transfer, role authorization, image-to-ticket attachment, signature confirmation, Redis state synchronisation and history co-failure. Each relationship relates to one project system. Role Authorization links a User-Role node with a WorkflowAction node in the form of an edge if the RBAC rule permits it. Image-to-ticket attachment links a field image with the ticket field obtained via OCR processing. Ticket transfer links the current work node with a subsequent node for approval or dispatching afterwards.

The Online Process is transformed into Graph States. When duty personnel generate a fault report, a ticket node will be added and linked with the following contents: alarms, suspected devices, service path. After the technical specialist verifies the fault, new connections are established between the tickets and candidate cables and repair information. When the responsible leader agrees to implement it, then role-authorisation-edges activate the following work-flow-state. During repairs at the site, field image nodes, signature nodes, and closure evidence nodes will be associated with tickets. The Graph Update Policy of this method enables it to consider fault locations as well as Workflow State simultaneously. It also holds other relevant audit information about the mobile repairs.

The standardised data fields of the repair ticket for graph construction. Mandatory items are as follows: Fault device unique identifier; Network topological position; Fault occurrence timestamp to the millisecond level standardization; Standardised fault phenomena; Affected services; Suspected cable section; Repair action; Work supervisor; Issuer; Approval status; Field image identification code; OCR extraction confidence value; Signature validity score; Closure Time. The mobile terminal may provide some part of the data in-field work, therefore each continuous and categorial feature is associated with an observation mask. If there is no image, absence of trace features or an untopology fields are presented as missing evidence instead of zeros. It needs to be handled because a zero-optical-power difference and no collected optical-power area indicate two different things.

A project-suitable dataset is built around the Digital Twin model of the mobile repair situation. There are 124 access Rings, 3,286 cable Sections, 5,913 Passive connection Points, 2,742 communication Sites and 4,812 service Paths in the topology component. The workflow includes the following six repair links: Fault report; Technical review; Leader approval; Repair dispatch; Field operation, ticket closure. The evidence part includes 18,240 controlled faults and 61,800 normal observation sequences. There are four kinds of faults: hard cable cut, high-loss bending, splice degradation and wrong patching. Each failure record contains information about the action taken, related images, as well as timestamped workflow data. This Design aligns the diagnosis task with the Project requirements of supporting fault localisation and repair ticket management simultaneously.

Table 1: Project Data Domains and Graph Mapping.

Data domain	Project source	Graph object	Main role
Communication topology	TMS2.0 resource database	Cable section, ODF, port, device, service path	Fault candidate and route reasoning
Repair workflow	TMS2.0 work-order database	Ticket, review, approval, dispatch, closure	Online process state and time measurement
Mobile field evidence	i State Grid mobile terminal	Image, OCR field, signature, operation timestamp	Evidence completeness and field verification
Telemetry and alarms	Communication monitoring platform	Alarm window, trace event, optical power feature	Fault symptom and timing evidence
Microservice state	Gateway, Redis, message service logs	API action, cache state, push event	Latency, synchronization, and deployment analysis

Table 1 shows the Data Domains involved in this model's construction. Figure 1 will be kept as the methods figure of project data organisation. Show how TMS2.0 resources, work orders, mobile evidence, telemetry and microservice log data can be converted into a heterogeneous repair graph structure. The figure is not directly generated here because Methods figures are handled as figure positions and Bohr one-click drawing instructions.

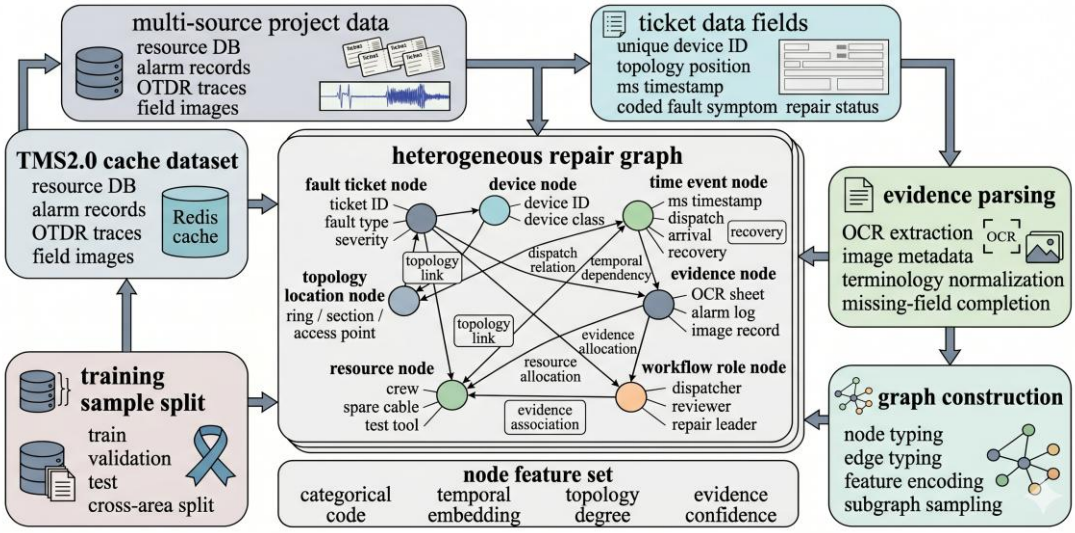

Figure 1: Project data organisation and heterogeneous repair graph construction.

Data quality control precedes graph construction. Only topologies that record have at least two adjacent segments, with a corresponding Service-Path reference and an exact distance value in the engineering area. Ticket record fault time, device ID, responsible person, current work process node. Only retain the field images that have associated OCR confidence scores or manual review status with the corresponding tickets. Signature records must ensure consistency across signers, roles, timestamps and ticket states. Records failing these checks are excluded from supervised training but preserved as data-quality cases for robustness evaluation.

The expansion of the candidate set conservatively. Each ticket includes all the parts that were crossed during path degradation, extended for 1 hop physically adjacent; Then added together ODF relationship history co-occurrence failures. To reduce the chance of excluding the real section due to temporary data staleness. The average candidate set comprises 49.2 sections, maintaining the ranking difficulty and compatibility for mobile device delays. All the graphs of baseline use a specific set.

For each reconstruction period, modify the work-flow Diagram again. Fault reporting adds alarm windows, affected devices and services, and duty-staff role. Add the following to candidate sections, topological neighbours, historical faults, etc., as technical reviews. Leader permission to activate authorisation lines, approve conditions. Add images of field execution such as signatures, OREs, trajectory paths and time-stamps. Closure Store final repair Position, Restoration Time; NLG Report Fields; Closure Signature. The same graph object therefore supports early diagnosis and post-repair review.

Ocr Is Conservatively Treated. Extracted fields are assigned confidence scores and linked to ticket fields; low-confidence items remain weak evidence and trigger manual confirmation. The NLG component only utilises verifiable or low-risk templates; thus, it is assessed based on reports being accepted and field completeness instead of fluency. Signature nodes encode account, role, timestamp, ticket state, trajectory, pressure variation, sampling density, and image compression ratio, not for fault localization but for workflow progression control. Events of microservices, such as authentication, API access, message push, Redis cache and file upload,

are also logged to assess the deployment lag and identify out-of-sync mobile states. When the mobile view and Redis state diverge, action recommendation is suspended until refresh.

2.2 Relation-Aware Localization and RBAC-Constrained Workflow Decision

The model has two coupled functions. The first function of topology location is to estimate the fault cable section and offset. The second function of Workflow Decision Support checks if the required pieces of evidence, roles and tickets are in place for moving on with repairs. These functions have been linked together because localisation candidates impact the dispatching and ticket content; The workflow status determines what type of evidence is available to be used by whom. Therefore, the proposed model employs relation-aware message-passing and an RBAC-constrained decision mask.

The initial node states contain type embeddings, project feature information, and evidence masks. Cable-section nodes include section lengths, topology degrees, service load counts, Optical trace details, historical co-occurrence failure scores, and distances to nearby surveillance stations. A ticket node includes ticket status, time passed; Role record, image number, field completion degree, approval outcome, closing basis information. A role node contains role type and permission group. An image-evidence node contains OCR confidence, extracted field type, compression ratio, and attachment time. A signature node includes the signer's role, vector trajectory length, pressure variations, timestamp and matching scores. These features are converted to the same-hidden-dimensional space before graph-propagation; then, relation-aware message-passing can be implemented as follows:

$$h_v^{(l+1)}=\sigma\left(W_0^{(l)}h_v^{(l)}+\sum_{r\in R}\sum_{u\in N_r(v)}\alpha_{uv}^{r,l}\left(W_r^{(l)}h_u^{(l)}+B_r^{(l)}e_{uv}^{r}\right)\right) \quad (2)$$

$h_v^{(l+1)}$ is the hidden state of Node v in Layer ℓ, ; $\sigma(\cdot)$ is the non-linear activation function; $W_0^{(l)}$ Is Self- State Transformation; $N_r(v)$ Is neighbor Set of v Under Relation r; $\alpha_{uv}^{r,l}$ Is relation attention weight;And $W_r^{(l)}$ and $B_r^{(l)}$ Are specific transformation Of Relation-Specific Transformations, And e_{uv}^{r} it Is Edge Feature Vector. relation-specific parameters are required for different scenarios of service traversal, ticket transmission, role verification, image addition, etc. A service-traversal edge can locate faults, and a ticket-transfer edge manages workflow information; A role-authorization edge restricts actions available to this user currently.

The attention term uses feature similarity and project-specific priors.

$$\alpha_{uv}^{r,l}=\mathrm{softmax}_{u\in N_r(v)}\left(\frac{(Q_r^{(l)}h_v^{(l)})\cdot(K_r^{(l)}h_u^{(l)})}{\sqrt{d}}+\gamma_r s_{uv}+\eta_r m_{uv}\right) \quad (3)$$

In this expression, $Q_r^{(\ell)}$ and $K_r^{(\ell)}$ are the relation query and key projections; d is the projection dimension; s_{uv} is the topology or workflow prior, such as inverse route distance, ticket-state compatibility, or service-path consistency; m_{uv} is the evidence availability mask; and γ_r and η_r are learned weights. To prevent the model from giving equal weight to a relation with incomplete evidence and one with no evidential basis at all. Also, the model can reduce the influence of physically similar cable sections on that part where there is no corresponding Service Path traversal.

Apply the RBAC restriction to workflow action evaluation scores. The project needs to perform dynamic role management; only after verification that the user has permissions for signing, approving, dispatching, closing a ticket will it be permitted. Therefore, the action probability is masked for workflow recommendation.

$$p(a \mid G_\tau)=\mathrm{softmax}(M_{\mathrm{RBAC}}(q,\rho,S_\tau) \odot o_a), \quad o_a=f_a([h_q^{(L)} \| h_\rho^{(L)} \| S_\tau]) \tag{4}$$

Here, $p(a \mid G_\tau)$ is the probability of workflow action a; $M_{\mathrm{RBAC}}(q,\rho,S_\tau)$ is the authorization mask for ticket node q, role node ρ, and workflow state q; $\odot$ is elementwise masking; o_a is the unmasked action logit; $f_a(\cdot)$ is a feed-forward action head; $h_q^{(L)}$ and $h_\rho^{(L)}$ are final hidden states of the ticket and role nodes; and $\|$ denotes concatenation. The mask is rule-based, and it originates from the project permission setting. The neural model cannot override the mask and thereby restrict high-scoring but unauthorized actions.

Fault-candidate-head determines the cable segment and offset; Workflow-head estimates the state of being ready for action. The common training target will be given next.

$$L=\lambda_1 CE(y,p_c)+\lambda_2 Huber(o_y,\hat{o}_y)+\lambda_3 BCE(b,\hat{b})+\lambda_4 CE(a,p_a)+\lambda_5 ECE(p_c) \tag{5}$$

Here, L is the total loss; λ_1 to λ_5 are loss weights; CE is cross-entropy; y is the true fault section; p_c is the candidate-section probability vector; $\mathrm{Huber}(\hat{o}_y, o_y)$ penalizes offset error between the true offset o_y and predicted offset $\hat{o}_y$; BCE is binary cross-entropy for the required evidence vector b and predicted evidence vector $\hat{b}$; a is the true workflow action; p_a is the workflow-action probability; and ECE is expected calibration error. The evidence term indicates whether there is sufficient image, signature, approval or closing-off evidence in a ticket. The calibration item has been retained, as the micro-application needs to determine whether to start auto-dispatching or maintain a ticket for manual review.

The model uses three relation-aware layers, 128 hidden units, four attention heads for major relation groups, and dropout of 0.15. Outputs a ranked list of cable-sections, offset estimate, ticket confidence, next-permitted workflow action, missing-evidence flags, and an edge-attribution map. Outside of the graph, OCR and NLG are not individualised modules. OCR confidence, as well as the obtained text information points; NLG reports serve as ticket-fulfilment criteria. Mobile signature characteristics are included in graphs as signatures-evidence nodes to evaluate their effectiveness on ticket availability independently of any physical faults.

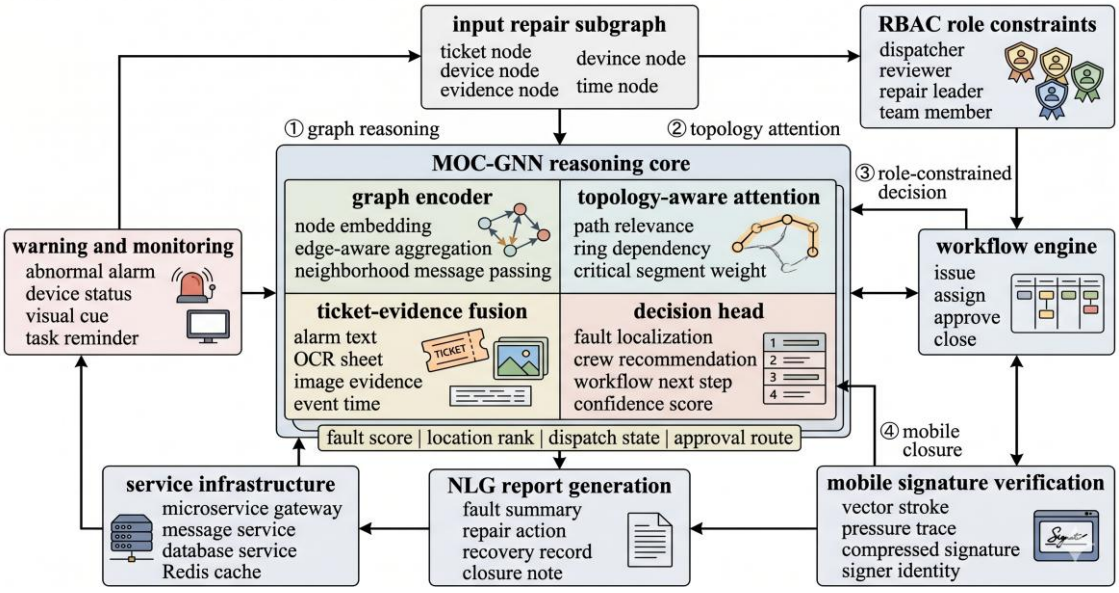

Figure 2: MOC-GNN localisation and RBAC-constrained workflow decison mechanism.

Figure 2 is reserved for the model mechanism. Show the central repair graph, relation-aware localisation, RBAC-constrained work-flow score, OCR / NNGevidence handling and mobile signature verification. Table 2 shows the base methods being compared with.

Table 2: Baselined methods and model predictions.

Method	Representation	Project data used	Output
Paper-ticket process	Manual offline process	Alarm and paper ticket	Dispatch route by manual judgment
Online form workflow	Electronic ticket	Ticket fields and approval state	Digital workflow without graph reasoning
Rule-based alarm correlation	Expert rules	Alarm, service path, reachability	Ranked candidate sections
CNN-OTDR	Trace-feature grid	OTDR-like features	Fault section class
XGBoost-fused	Tabular feature vector	Topology, ticket, OCR, telemetry features	Fault section class
GAT	Homogeneous graph attention	Topology and alarm graph	Fault section class
R-GCN	Typed-edge graph	Topology and service relations	Fault section class
HGT	Heterogeneous graph	Typed nodes and edges	Fault section class
MOC-GNN	Project repair graph	Topology, ticket, role, OCR, NLG, signature, telemetry	Fault section, offset, next permitted action

Separation of action recommendation and automatic execution. The model recommends the following operations: dispatch, review, signature collection, closure, and additional evidence; After that, it will be processed in accordance with the workflow engine based on permissions. This Design maintains Dynamic Authorisation: high localisation confidence can ensure the preparation of dispatch, but a missing Issuer Signature will prevent completion. The graph provides supporting Evidence and rank candidates; The workflow engine implements institutional Rules.

Interpretation is based on relation-group masking and changes in the probabilities of the selected candidates or actions. A large drop after masking service traversal indicates service-path dependence; a drop after masking image attachment indicates the need for field-image confirmation; a change after masking RBAC edges indicates permission sensitivity. To enhance the interpretability and control of over-fitting, relations are organised into different types: Physical objects, Services; Workflow steps; Permission relationships; Evidence information. Thus, enabling the model to make topological-based, workflow-based and evidence-type decisions.

An offset head is retained because repair crews need a local inspection region rather than section classification alone. Estimate its position in the chosen part based on candidate-state feature, local trace signal, route distance to monitored point and field evidence availability. Training uses only events with known repair positions; for wrong patching, the target is aligned to the patching or ODF location rather than a cable break.

Furthermore, it generates a missing-evidence vector to predict whether the ticket needs photo evidence, written testimony, topology identification, Service-Path inspection, or need manual technical review. Improving Mobile Interaction is realised by identifying the field

preventing workflow advancement, which does not return a probability but an identification result directly. Mainly calibrated at the stage of selecting models via a joint criterion incorporating aspects such as localisation, evidence-fulfilment, work-flow-actions, and calibration loss functions; Only post-calibrated with temperature-scale after.

2.3 Cross-Area Evaluation Protocol and Project Metrics

Test whether this system enhances physical faults location and mobility-based repair management compared with previous systems. Cross-topology area distribution of the data set. Four areas are trained in turn; One will be validated after that; And then we shall perform tests on all of them subsequently. This division prevents almost the same cable neighbourhoods from appearing during training and testing. The workflow log is combined with the corresponding topological area; therefore, it needs to generalise for a new combination involving topology density, service path, and role action.

Baselines include the repair workflow, feature fusion and Graph Learning. The first baseline of the paper-ticket process involves manually analysing alarms and circulating offline tickets. Only for the comparison of Workflow's Time and Completeness. The second reference case is a non-graph-structured form of the online system. Digitise the ticket, but maintain localisation through rule-based alarm linkage. The third baseline is CNN-OTDR, which uses trace-derived features and ignores repair workflow. The fourth baseline of XGBoost-fused uses engineered topology, alarm, OCR and ticket features to build a tabular model. The graph-baseline models are GAT, R-GCN and HGT. All of them belong to the same train-validation-test fold system. Graph-based baseline receives the same candidates but does not utilise a RBAC-constrained action mask unless otherwise mentioned;

We have carried out the evaluation of localisation through the adoption of Top-1 accuracy, Top-3 accuracy, Macro-F1, median localisation error, and 95th-percentile localisation error. The work flow performance was measured through the time from ticket receiving to dispatching, the ticket item completing percentage, the unauthorized behavior refusing percentage, the average API delay time, the evidence verified closing percentage, and the report producing accepting percentage. Calculation of localisation error was carried out from two aspects: whether the cable section that was predicted matched the section that was true, and the offset deviation which existed inside the selected section. When the prediction of the section was correct, the error was only determined by the difference of offset. When section prediction was not correct, an extra route-distance punishment was added to express the physical distance gap between the real and forecast cable sections. This definition makes that a section-level error that is close and a misassignment that is over a long distance are not handled as same things.

Organise robustness tests based on project risks. The first risk is an incomplete topology or resource data: remove or reconnect the service traversal edges. Risk two: Incomplete mobile evidence; simulating this through masked OCR fields, missing field pictures, or invalid signatures. The third risk is telemetry incompleteness, simulated by masking optical and alarm features. Fourthly, the microservices failure test involves adding multiple simultaneous tickets and APIs for simulation. Only the test folds are affected by each perturbation, as indicated below. This Design verifies if the trained system is stable under the actual condition of low-quality training data in mobile repair.

Abstraction tests sequentially omit one function at a time: service-path relationship, ticket-transfer relationship, RBAC operation mask, OCR evidence node, NLG report-completeness objective, mobile-signature feature, Redis state feature, calibration term. Re-train each ablation model on different fold data simultaneously. The Ablation analysis report localisation accuracy, 95% Error, Ticket dispatch Time, Evidence Completeness, Unauthorized Action Rejection.

Figure 3 is a reserved evaluation protocol Figure; It includes the Cross-area Split, Project Data Domains, Baseline Groups, Perturbation Settings, Ablation Loop and Metrics.

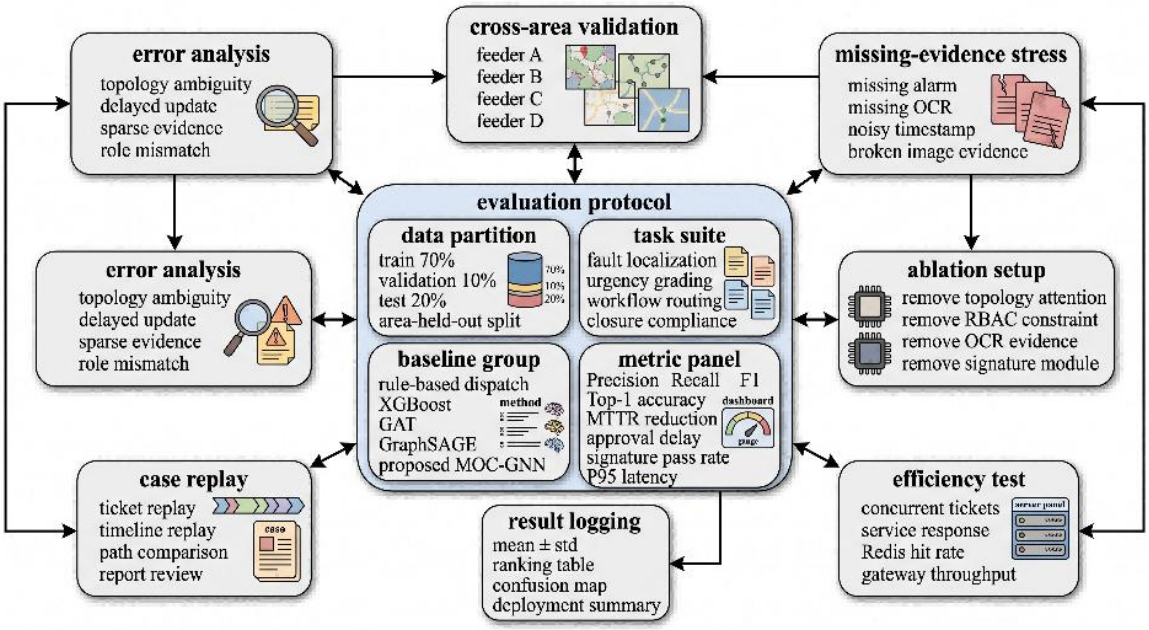

Figure 3: Cross-sector Evaluation Protocols for Localization and Mobile Workflows Validation

Tuning the number of hidden nodes within [64, 128, 256] range; LAYERS: (2-4) x times; Dropout rates in [0.05, 0.15, 0.25]. The final model has 128 hidden units in three layers without using dropouts. The loss weight was set to 1.0 for the classification of section type, to 0.35 for offset prediction; To 0.20 for evaluation standardization, 0.25 For workflow action classification And calibrated by holding It stable In all test fold cases.

Efficiency of workflow at each stage was measured rather than in terms of overall time. Paper tickets include manual collection, technical comparison, offline approval, dispatch preparation and other contents; The online form eliminates paper circulation but still follows rule-based localisation; Graph-aided micro-applications add candidate rankings and missing evidence suggestions. Identify whether the time-saving benefits originate from approvals, localisations or field confirmations.

Report Generation is evaluated based on Field Completeness and Report Acceptance. The extent to which mandatory repairs have been recorded before closing inspection; Report acceptance refers to the part of generated drafts without significant manual corrections; Report Rejection is triggered when there are errors such as incorrect device identifiers, topological positions, unsuitable fault causes, missing signatures, and unverified field images. Authorization checked whether the action violated or passed based on an unauthorised-Action-Rejection model and a valid-Action-Pass metric to avoid interference with authorised repair activities.

Under 50-1,000 concurrent repair tickets, the microservices' performance indicators included API latencies, response rates, cache hit rates, state-change delays, etc. Image upload, as well as pre-processing for OCR technology, were all parts of the mobile repair system. While recording inference time in isolation for this study, we will analyse the entire process from receiving requests to submitting results by end-to-end testing.

3 Results and Discussion

3.1 Localization Accuracy and Online Repair Workflow Effect

The first Result Group aims to investigate if Graph-Assisted Localisation affects the repair effect in mobile micro-Applications. Physical localisation metrics and workflow times are compared here; a faulty candidate can be of no use if it increases travel time beyond that of an untested item. Table 3 and Figure(s) 4-5 show the overall results obtained from this experiment.

Table 3: Localisation and workflow performance in six cross-areas of tests.

Method	Top-1	Top-3	Macro-F1	Median error (m)	P95 error (m)	Ticket-to-dispatch (min)	Completeness
Rule-based alarm correlation	0.682	0.819	0.661	352	964	38.5	0.711
CNN-OTDR	0.784	0.902	0.762	218	616	31.4	0.724
XGBoost-fused	0.847	0.934	0.824	164	482	22.6	0.839
GAT	0.891	0.958	0.869	132	388	18.9	0.874
R-GCN	0.903	0.964	0.882	119	356	17.5	0.892
HGT	0.916	0.972	0.899	107	319	15.8	0.914
MOC-GNN	0.938	0.984	0.924	78	226	11.6	0.964

Table 3 shows that rule-based alarm correlation reaches 68.2% top-1 localization accuracy and has a 95th-percentile error of 964 m. Because CNN-OTDR can reach an accuracy of 78.4% through trace morphology, although the 95th percentile error is still at 616 meters and cannot be distinguished from other paths; Using XGBoost-fused achieves an accuracy of 84.7%, but it fails to propagate the evidence via cable-section neighbours and workflow relationships. GAT, R-GCN, and HGT increase the result from 89.1%, 90.3% and 91.6% respectively. MOC-GNN reaches 93.8% top-1 accuracy, 98.4% top-3 accuracy, 92.4% macro-F1, 78 m median localization error, and 226 m 95th-percentile error. A decrease in the tail error is necessary for this reason: while the region being studied may exceed one of its cables by a certain degree, it currently also contains another branchline closeby.

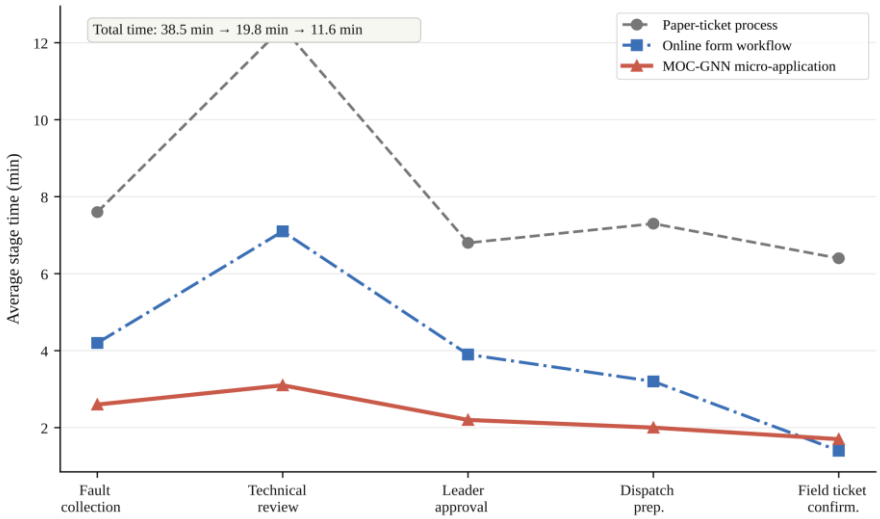

Figure 4: Reduced Stage-level maintenance workarounds Time.

As shown in Figure 4, the workflow comparison. On average, all parts of producing and distributing the paper tickets take around 38.5 minutes. Without graph reasoning, the time of 30 minutes would only reach 19.8 due to the digitisation of ticket delivery reminders; The proposed mobile micro-application with graph-assisted localization reduces the time further to 11.6 min. As shown in Figure 4 below: Fault Collection; Technical Review; Approval; Dispatch Preparation; Field Ticket Verification. The biggest decrease is at the technical acceptance stage; it takes 12.4 minutes according to previous methods but only 3.1 using MOC-GNN. It is in accordance with this model's output; The technical specialist receives a sorted list of cables and sections, offset estimation, confidence score, as well as a warning for missing evidence.

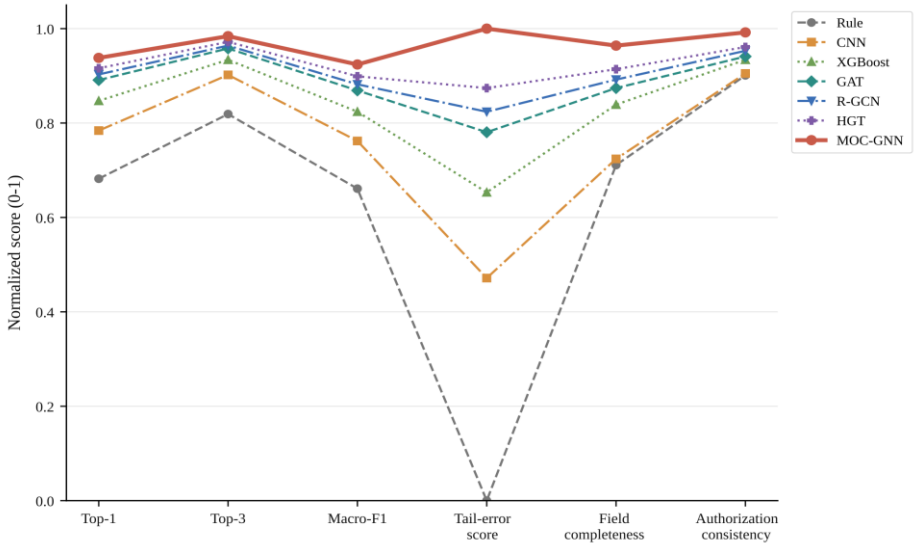

Figure 5: Normalised localisation, Workflows and decision-quality of compliance.

As shown in Figure 5, MOC-GNN has the highest Normalized Performance across Localisation, WorkFlow and Compliance Metrics. Its strengths compared to HGT are field coverage and the consistency of authorisation; since HGT only captures topological structure without considering RBAC restrictions or evidence-completed targets. Therefore, the gain does not come from individual fault identification or workflow preparedness but rather jointly from both aspects.

At the fault-class level, hard cut achieves the highest top-1 accuracy (97.2%) among various classes; then come mispatching (94.5%), high-loss bending (91.8%), and splice degradation (90.4%). The two soft-failure classes exhibit the greatest tail error, but their top-3 accuracy exceeds 96.3 per cent. Even when top-1 is wrong, 71.8% of true sections are adjacent to or share an ODF with a top-3 candidate, so the field search usually remains local.

Workflow Improvements are Also Notable. Ticket completeness increases from 82.1% to 96.4%, report acceptance rises from 78.6% to 91.7%, and unauthorized-action rejection reaches 99.2%. The technical review time can be shortened from 7.1 minutes to 3.1 minutes by generating the candidate sections and missing-evidence prompts automatically. These indicators all improve as a whole; therefore, it can provide some ideas for related applications in other domains.

Figure 5 also shows the model boundaries. HGT still holds a leading position in terms of topology characteristics, such as the first-place Accuracy at top-3. XGBoost-fused handles ticket fields but lacks message passing and shows larger tail localization error. MOC-GNN is superior to both because it incorporates topological, ticket-evidence and workflow constraint graphs at once.

3.2 Robustness, Ablation, and Evidence Completeness

The second result Group examines Robustness and Module Contribution. This section is essential as the project's data source materials have multiple characteristics; that is to say, incomplete recordings from TMS2.0; unclear field images; signatures collected via various devices; and tele-measurement contents lagging behind in time. As shown in Figures 6-8 below, how the model performs under these circumstances.

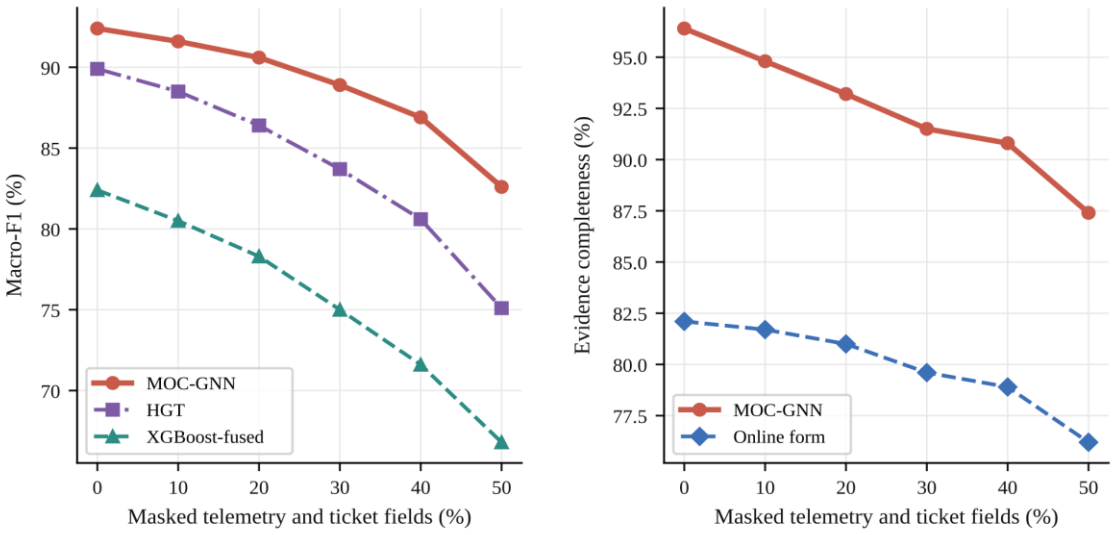

(a) Localization robustness

(b) Ticket evidence completeness

Figure 6: Robustness to missing telemetry data and tickets.

Figure 6 presents the results of missing evidence. When 20% of telemetry and ticket fields are masked, MOC-GNN retains 90.6% macro-F1, while HGT decreases to 86.4% and XGBoost-fused decreases to 78.3%. The MOC-GNN achieves an 86.9% macro- F1@MR=40; , and HGT drops to less than 80.6%. Similarly, according to the ticket-completeness curve data; At 40% masking, MOC-GNN still reaches 90.8% evidence completeness after prompting for missing OCR, image, or signature fields, whereas the online form workflow stays at 78.9%. Due to the evidence-completeness goal of the training loss, this difference arises. The model is not limited to classifying a fault but also learns which evidence objects should be present in a correct repair ticket.

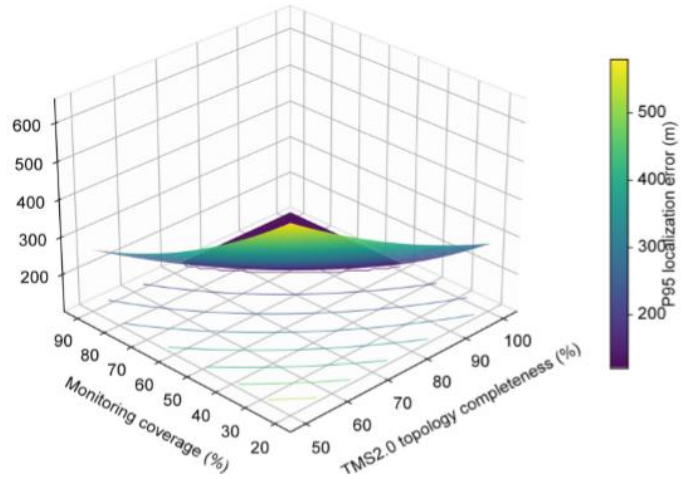

Figure 7: Error Surface of three-dimensional positioning with TMS2.0 topology completeness and coverage.

Figure 7 shows the three-dimensional localisation surface under topological completeness and coverage of monitoring. TMS2.0 topological completeness less than 70% or monitoring coverage below 35%; The 95th percentile localisation error greater than 520m. A topological completeness level reached 95% and coverage reached over 70%; The deviation was within ±190 metres. Various levels of topological data quality detection are mutually reinforcing with each other. High monitoring coverage cannot fully compensate for wrong service-path records, while complete topology does not fully solve weak soft-failure detection when optical evidence is missing. Based on this, there is an applicable practical reference point for inventory re-organisation in conjunction with the monitoring-point plan to enhance mobile repair accuracy.

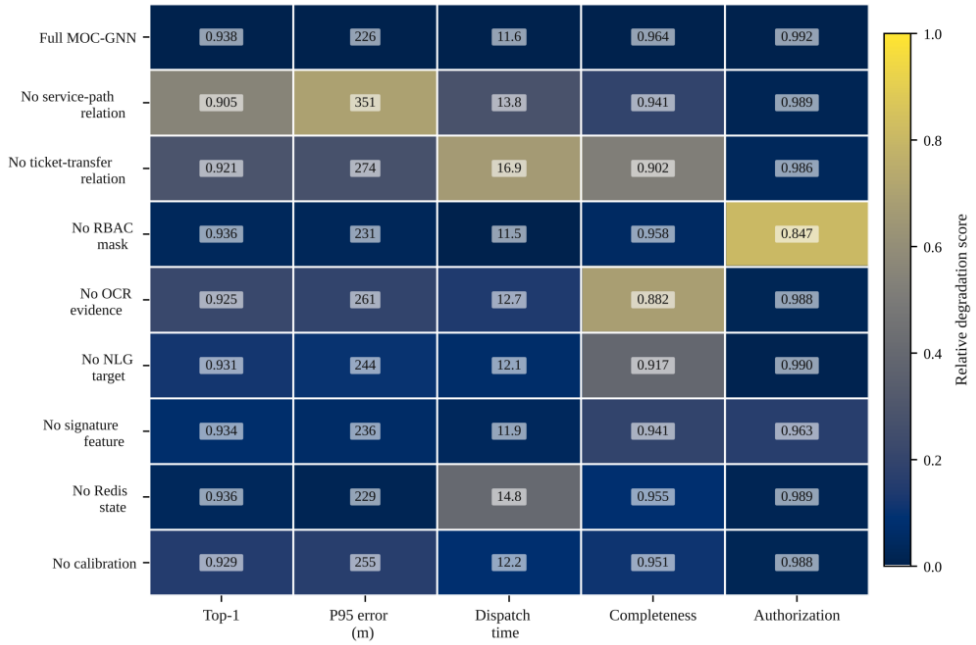

Figure 8: Module ablation heatmaps of localisation, Workflows Time, Completeness and Authorisations.

As shown in Figure 8, modules' effects are not interchanged but taskspecific. After removing the service-path relationship, the top-1 accuracy dropped to 93.8%, while losing 95

per cent error at 226m up; It was found that topological structures dominated location. Removing the RBAC mask moderately improves fault prediction but severely increases unauthorized-action rejection; It cannot meet the requirements of control repair. Removing OCR evidence nodes cuts ticket completeness from 96.4% to 88.2% and report acceptance from 91.7% to 82.5%. Removing the NLG completeness target mainly weakens report acceptance and closure consistency, whereas removing Redis state features increases latency and slows ticket-state refresh. Therefore, the ablation boundaries are as follows: Service-Path and Topology Relation Support Localization; RBAC and Signature Function Supports Compliance; Ocr and NLG Features Can Improve Field Completeness and Report Quality; Redis State Information Provides Responsiveness.

Robustness results show that stale service-path records are the most harmful data defect. At 20% service-path edge noise, top-1 accuracy falls to 86.7% and probability calibration deteriorates. Weak soft failures are still challenging in sparse monitoring and missing field evidence. In the fifth-low uncertainty group, the top-1 accuracy was 81.9%, but it dropped to 94.1%; under 50% of missing telemetry and ticket fields, macro-F1 decreased to 82.6%, but the top-3 accuracy reached 91.3%. These should not be classified as assistance diagnosis but automatically dispatched. See Figure 7; No monitoring is unable to cover a missing topology, nor can an entire topology completely eliminate sparseness in detection. A low-error region should have synchronised TMS2. 0 service-path data and ample monitoring scope.

Therefore, the deployment Policy will be conservative. First, service-path relations and topology completeness need to be determined; otherwise, it cannot determine which part is repairable. Before enabling the automatic dispatch or close recommendation, RBAC masking and signature verification need to be set up. OCR and NLG can then reduce manual reporting, but only under confidence control. The threshold test confirms that this policy has been successful; under the condition of restricting Automatic Dispatch at least 13% probability events with Entropy calibration scores lower than a specific value, around 69.5% of all tickets require no further human supervision for selection. Raising the threshold to 0.65 can increase the coverage rate to 84.2%, but top-1 error is 92.6%, and the 95th percentile of errors reaches 302m. The more stringent requirement.

3.3 Microservice Deployment and Case-Level Repair Traceability

The third Result Group is deployment in the mobile micro-app architecture. The project should have a three-layer flexible technical architecture of mobile presentation, microservice Gateway, application service, base service and data service. Therefore, the model needs to run under an API Gateway, use a uniform login interface, retrieve data from TMS2.0, modify Redis state, respond promptly via mobile devices, etc.

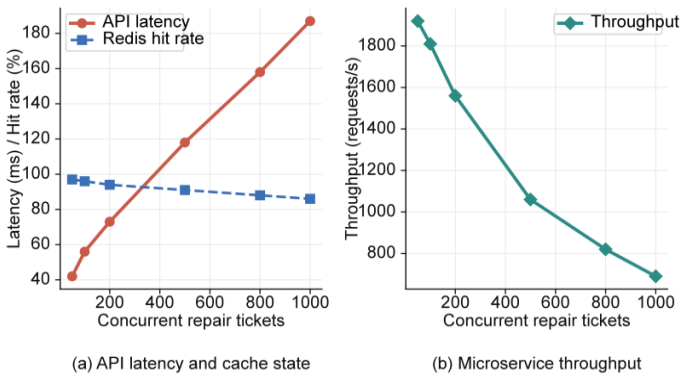

Figure 9: Microservice Scalability for Concurrent Repair Tickets.

See Figure 9: Scalability of Repair Ticket Concurrency. At 50 ticket loads, the average API latencies were 42ms; At 50 tickets, this latency reached 118MS, with a throughput of approximately 1920requests/Ms; After adding another 50 tickets, the delay increased to about 187Ms. The Redis cache hit rate stays above 91% up to 500 tickets and declines to 86% at 1,000. These results support the ticket-level decision-making aid for mobile repair. When the load is high, mainly delays due to cache refreshing, image upload, OCR pre-processing and workflow state synchronisation; not graph inference. This pattern fits with the System Design: Gateway for Authentication and API Access; Application Service that executes Graph Inference and Workflow Scoring; Base Service responsible for managing Cache and Messaging; Data Layer to read TMS2.0 Topology and File Records; The deployment optimisation should be focused on Asynchronous Image Handling, Cache-Refresh Policy and Message-Delivery Reliability.

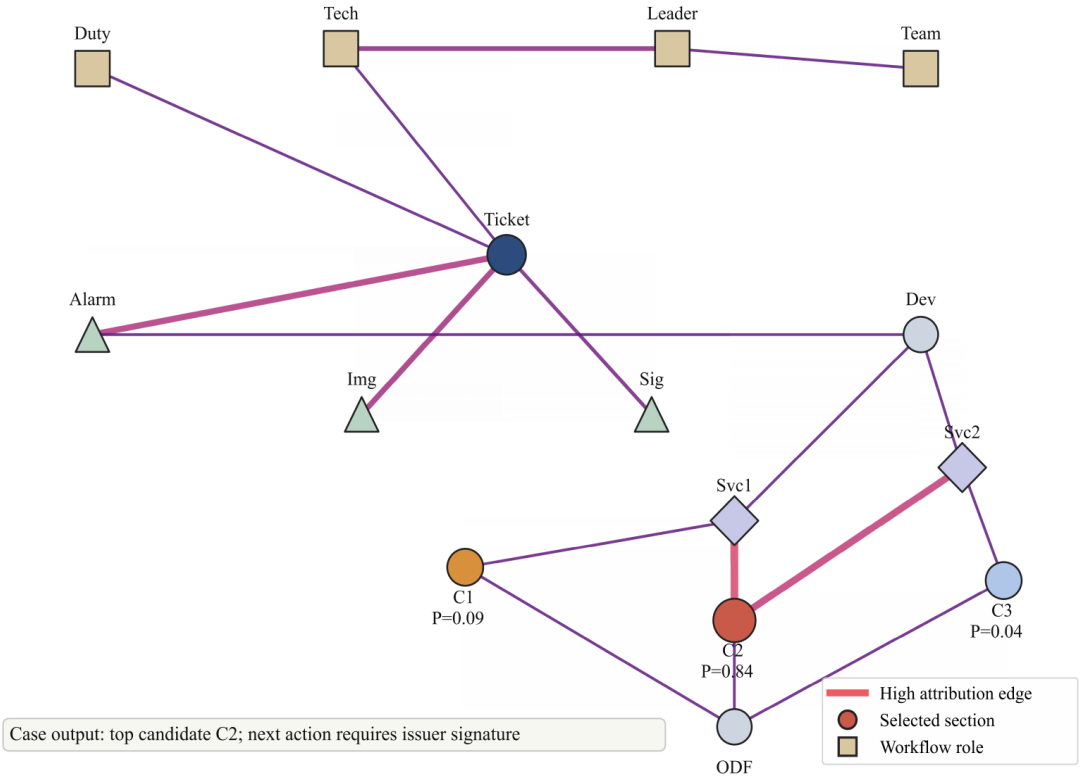

Figure 10: Case-based repair of graphs using candidate probabilities and workflow-action state information.

Figures 10 trace the repair ticket. Although the initial alarm appears at a downstream device, in fact, it is a severe loss-induced bending event occurring in an uplink-optical-cable segment serving two impaired-service paths. Rule-based correlation sorts the downstream branch first; MOC-GNN gives a probability of 0.84 for the upstream cable segment, 0.09 for the adjacent same-shielded segment, and only 0.04 to the downstream branch. Service traversal, local trace deviation, ticket image evidence, and alarm propagation all participate in this attribution. Due to an invalid signature of the issuer, directly completing can be blocked, and it will be forwarded for technical review and leadership approval. Combined Output shortens the inspection distance from 1.3 kilometres to 210 metres. After uploading the field image and completing the pressure-aware signature, the ticket will be ready to close; at this time, the NLG module will generate a repair record. Therefore, the repair graph can support localisation, work flow control and traceable explanations in a single structure.

Dependence of deployment on data governance, rather than model scoring. Localisation accuracy depends on the synchronised topology, work-order status, service-path mapping and role information. Unupdated traversal relations may cause fault attribution; unsynchronized RBAC tables affect authorisation; low OCR confidence needs to raise a report-review issue. In practice, high confidence tickets are automatically issued; Uncertain Tickets display a list of the top three options, missing-Evidence warnings, and relationship inference information in real-time. Each closed ticket creates a graph trace for predicted and corrected sections, repair operations, personnel information, associated pictures or reports, etc., providing reference for updating co-defect relationships, identifying loose data connections, and assisting with future auditing and optimisation; directly retrieve the stored graph instead of reconstructing it based on scattered forms and call logs.

4 Conclusion

Based on this, the mobile-optical-cable-communication fault-repair-oriented-MOC-GNN framework was designed in an example situation. The framework transforms TMS2.0's resources, work orders, mobile evidence, telemetry data, signatures, roles/permissions, microservices status into a hybrid repair graph. The graph can achieve fault localisation and mobile-workflow decision-support functions.

(1) The data organisation model associates repair tickets with physical topology information. Cable Sections, Service Paths, Devices, Workflows' Nodes, Roles, OCR Fields, NLG Report Fields, Signature Samples are all treated as interconnected graphs. The Design of this system can simultaneously retain topological evidences and processing data within a single diagnostic framework.

(2)The relation-aware graph model enhances the repair-oriented localisation and workflow quality. The proposed method reaches 93.8% top-1 accuracy, 98.4% top-3 accuracy, 78 m median error, and 226 m 95th-percentile error. The average waiting-time-to-delivery is reduced by 76.4 per cent compared with that for tickets processed using the paper system; Field completeness increased to 96.4%.

(3)Still based on the quality of topological and workflow data. Stale Service-Path Records, Sparse Monitoring Coverage, Low-Quality Field Images, and Unsynchronised Role Tables will Reduce Reliability. Future work should validate the model with live repair tickets, update topology and permission relations after work-order closure, and extend the method to simultaneous multi-fault events and cross-area emergency repair.

The essential values are as follows: Firstly, by integrating a mobile work flow object with an indivisible repairing physical Object. This link can make the model's output affect fault diagnosis, work order review, operation permissions, and post-repair analysis results.

Additionally, it establishes a Boundary for Deployment. Only use automatic dispatch when the topological record, monitoring evidence and ticket evidence have been fully collected. Under high uncertainty, the system should present ranked candidates and missing-evidence prompts for assisted diagnosis.

Under this scheme for the present work, the proposed realisation path includes: firstly deploying graph-aided ranking at an assisted-diagnosis level; Secondly, enabling high-confidenceself-automatic-dispatch function when topoligry records role table mobile-evidence acquisition verification have completed pilots operation.

This path keeps the first deployment conservative while still using the model to reduce manual search work and improve evidence quality.

It needs field verification to optimise the setpoints of these parameters in detail.

Funding

This work was supported by the Science and Technology Project of State Grid Sichuan Electric Power Company: Research on Micro-application Technology for Mobile Optical Cable Communication Fault Repair Management (No. 521910250001).

About the Author

Weishan Zhao had his birth place in Zhangye, Gansu Province, China, in the first month of 1989. He obtained his graduation from Sichuan University in July of 2013, and at the present time he holds a work position at State Grid Zigong Electric Power Supply Company. The research direction of him is the electric power communication.

Puyu Liu took birth in Zigong, which belongs to Sichuan Province, China, in the June of 1993. He obtained his graduation diploma from Southwest Jiaotong University in the June of 2019, and at the current time he holds a work position at State Grid Zigong Electric Power Supply Company. The research directions that he engages in include power system communication and data application analysis.

Ming Li, who was given birth in July 1990, has his birth place at Yibin, which belongs to Sichuan Province, China. He obtained his graduation from Chengdu University of Technology in the June of 2017, and at present he holds a work position at State Grid Zigong Electric Power Supply Company. The research direction which he carries out is the power domain communication.

Yong He took birth in Zigong, which lies in Sichuan Province of China, in November 1988. In June 2013, he obtained his graduation from the Sichuan University of Science & Engineering, and at the present stage, he holds a work position at the State Grid Zigong Electric Power Supply Company. The research interest of him is the communication in electric power field.

Songjia Liu was given birth in August 1996, at Guangyuan City which is located in Sichuan Province, People’s Republic of China. He obtained his graduation from Southwest University of Science and Technology in the June of 2022, and at present he holds a work position at State Grid Zigong Electric Power Supply Company. The direction of his research work is artificial intelligence.

References

[1] Cruzes, S. (2024). Failure management overview in optical networks. IEEE Access, 12, 169170–169193.

[2] Musumeci, F., & Tornatore, M. (2025). Failure management in optical networks with ML: A tutorial on applications, challenges, and pitfalls [Invited]. Journal of Optical Communications and Networking, 17(8), C144–C155.

[3] Wang, D., Zhang, C., Chen, W., et al. (2022). A review of machine learning-based failure management in optical networks. Science China Information Sciences, 65(11), 211302.

[4] Li, Z., Zhao, Y., Li, Y., et al. (2021). Fault localization based on knowledge graph in software-defined optical networks. Journal of Lightwave Technology, 39(13), 4236–4246.

[5] Xu, X., Chen, H., Simsarian, J. E., et al. (2023). Optical network diagnostics using graph neural networks and natural language processing. In Optical Fiber Communication

Conference (p. M3G.5).

[6] Karunakaran, V., Romero Reyes, R., Shariati, B., et al. (2025). Dynamic network-aware soft failure localization using machine learning in optical networks. Journal of Optical Communications and Networking, 17(11), 1032–1046.

[7] Chen, X., Chen, X., & Zhu, Z. (2025). Interpretable optical network fault detection and localization with multi-task graph prototype learning. Journal of Optical Communications and Networking, 17(9), D73.

[8] Rusek, K., Suárez-Varela, J., Almasan, P., et al. (2020). RouteNet: Leveraging graph neural networks for network modeling and optimization in SDN. IEEE Journal on Selected Areas in Communications, 38(10), 2260–2270.

[9] Ferriol-Galmés, M., Rusek, K., Suárez-Varela, J., et al. (2022). RouteNet-Erlang: A graph neural network for network performance evaluation. In IEEE INFOCOM 2022. 2018–2027.

[10] Suárez-Varela, J., Almasan, P., Ferriol-Galmés, M., et al. (2023). Graph neural networks for communication networks: Context, use cases and opportunities. IEEE Network, 37(3), 146–153.

[11] Matzner, R., Luo, R., Zervas, G., et al. (2023). Intelligent performance inference: A graph neural network approach to modeling maximum achievable throughput in optical networks. APL Machine Learning, 1(2), 026112.

[12] Savva, G., Panayiotou, T., Tomkos, I., et al. (2022). Deep graph learning for QoT estimation of unseen optical sub-network states: Capturing the crosstalk impact on the in-service lightpaths. Journal of Lightwave Technology, 40(4), 921–934.

[13] Sandhu, R. S., Coyne, E. J., Feinstein, H. L., et al. (1996). Role-based access control models. IEEE Computer, 29(2), 38–47.

[14] Li, M., Lv, T., Chen, J., et al. (2023). TrOCR: Transformer-based optical character recognition with pre-trained models. In Proceedings of the AAAI Conference on Artificial Intelligence, 37(11), 13094–13102.

[15] Dong, C., Li, Y., Gong, H., et al. (2022). A survey of natural language generation. ACM Computing Surveys, 55(8), Article 173.

[16] Schuster, F., Zimmermann, A., Ntentos, E., et al. (2024). Modeling microservice architectures. Journal of Systems and Software, 216, 112041.

[17] Shen, S., Han, J., Bardhi, K., et al. (2025). Unified monitoring and telemetry platform supporting network intelligence in optical networks. Journal of Optical Communications and Networking, 17(2), 139–151.

[18] Zakrzewski, Z., Głąbowski, M., Zwierzykowski, P., et al. (2024). Optical technologies supporting 5G/6G mobile networks. Photonics, 11(9), 833.

[19] Kipf, T. N., & Welling, M. (2017). Semi-supervised classification with graph

convolutional networks. In International Conference on Learning Representations.

[20] Veličković, P., Cucurull, G., Casanova, A., et al. (2018). Graph attention networks. In International Conference on Learning Representations.

[21] Schlichtkrull, M., Kipf, T. N., Bloem, P., et al. (2018). Modeling relational data with graph convolutional networks. In The Semantic Web, ESWC 2018 (Lecture Notes in Computer Science, Vol. 10843, 593–607.

[22] Hu, Z., Dong, Y., Wang, K., et al. (2020). Heterogeneous graph transformer. In The Web Conference (pp. 2704–2710).

[23] Zhang, C., Chen, Y., Zhang, M., et al. (2025). SHAP-assisted EE-LightGBM model for explainable fault diagnosis in practical optical networks. Journal of Optical Communications and Networking, 17(2), 81–94.

[24] Behera, S., Panayiotou, T., & Ellinas, G. (2023). Machine learning framework for timely soft-failure detection and localization in elastic optical networks. Journal of Optical Communications and Networking, 15(10), E74–E85.

[25] Wu, H., Hu, Q., Cai, Z., et al. (2025). Machine learning-aided hierarchical framework for proactive inline EDFA gain degradation detection and localization in optical networks. Journal of Optical Communications and Networking, 17(12), 1082–1093.